



Cite this: *Sustainable Food Technol.*,  
2026, 4, 1633

# Biodegradable films based on alfalfa cellulosic residue and carrageenan blends for sustainable food packaging

Sandeep Paudel  and Srinivas Janaswamy \*

Plastic remains a dominant packaging material, but its non-biodegradability poses significant environmental and health concerns. Although starches, proteins, and lipids offer biodegradable alternatives, their primary role in food security necessitates exploring other sources. In this context, cellulosic residues from biowaste provide a promising option. This study examines the development of biodegradable packaging films from alfalfa cellulosic residue and investigates how their mechanical properties are improved through complexation with carrageenans. Alfalfa cellulosic residue (ACR) was extracted using alkaline and bleaching treatments, dissolved in 68%  $\text{ZnCl}_2$ , and then complexed with iota- ( $\iota$ ), kappa- ( $\kappa$ ), and lambda- ( $\lambda$ ) carrageenan solutions at concentrations of 0.5%, 1%, and 1.5%. The solutions were further crosslinked with calcium ions and plasticized with sorbitol, yielding nine different ACR-carrageenan films, with the ACR film serving as the control. The films were characterized for mechanical properties, water vapor permeability (WVP), color, UV-Vis-IR transmittance, water solubility, hydrophobicity, water uptake kinetics, antioxidant activity, and soil biodegradability. Incorporating carrageenan significantly increased tensile strength from 16.9 to 29.9 MPa, but decreased elongation at break, with a subtle effect on WVP. Water solubility and absorption increased by 20.1% and 173.9%, respectively, in the ACR- $\lambda$ 1.5% films. Water uptake followed Peleg's kinetics, while soil biodegradation exhibited second-order kinetics and reached complete degradation within 40 days at 24% soil moisture. These results demonstrate the potential of ACR-carrageenan films as innovative biodegradable packaging materials, offering an eco-friendly alternative to plastics in food packaging, promoting sustainability and a circular bioeconomy, and creating new income opportunities for alfalfa farmers.

Received 31st October 2025  
Accepted 5th December 2025

DOI: 10.1039/d5fb00872g

rsc.li/susfoodtech

## Sustainability spotlight

The ongoing reliance on petroleum-based plastics poses significant environmental issues, emphasizing the urgent need for sustainable packaging alternatives. This study investigates the use of alfalfa cellulosic residue, a widely available agricultural byproduct, as a renewable source of cellulose for biodegradable films. By blending alfalfa-derived cellulose with  $\iota$ -,  $\kappa$ -, and  $\lambda$ -carrageenan, composite films with improved mechanical strength, barrier properties, and UV-blocking capabilities have been developed. These films achieved complete biodegradation within 40 days under conditions of 24% soil moisture. By converting agricultural waste into valuable resources and combining it with natural biopolymers, this work presents a promising approach to developing high-performance. These eco-friendly packaging materials promote sustainability and the circular bioeconomy.

## 1. Introduction

Most plastic packaging materials are classified as single-use plastics, designed for a single application before being disposed of, incinerated, or abandoned, and over half of them fall into this category.<sup>1</sup> Due to their resistance to biodegradation, these materials persist in the environment for longer durations, with nearly half of the plastic debris in marine ecosystems consisting of single-use items.<sup>2-9</sup> It is estimated that the world's oceans contain approximately 5.25 trillion plastic

particles, weighing around 269 000 tons.<sup>10</sup> As plastics degrade, they fragment into micro- and nano-sized particles that have become ubiquitous in terrestrial and aquatic environments.<sup>11-16</sup> Humans are therefore at significant risk of exposure to these tiny particles, mainly through the consumption of seafood. Additional sources include food and beverages packaged in plastic containers.<sup>14,17</sup> For example, a study found microplastic contamination in 93% of bottled water samples.<sup>18</sup> Alarmingly, microplastics have also been detected in human tissues, including the placenta, lungs, and brain.<sup>19-21</sup> Beyond physical contamination, chemicals leaching from plastics pose further health risks.<sup>4,22</sup> Compounds such as bisphenol A, phthalates, styrene, vinyl chloride, flame retardants, and other additives

Department of Dairy and Food Science, South Dakota State University, Brookings, SD 57007, USA. E-mail: Srinivas.Janaswamy@sdsu.edu



have been associated with cardiovascular diseases, cancer, congenital abnormalities, and developmental disorders.<sup>17,23,24</sup> Given the profound environmental and health consequences of plastic packaging, there is an urgent and unmet need to develop biodegradable, non-toxic, sustainable, and renewable alternatives.

In this context, natural biopolymers such as cellulose, chitosan, starch, lignin, and proteins have attracted significant attention as sustainable alternatives due to their inherent biodegradability.<sup>25–28</sup> Cellulose, a highly abundant and renewable polysaccharide, is valued for its rigidity, strength, and non-toxicity.<sup>29,30</sup> There are some studies on cellulose-based films, such as microcrystalline cellulose,<sup>31</sup> corncob cellulose,<sup>32</sup> soyhull cellulose,<sup>33</sup> cow dung cellulose,<sup>34</sup> grapevine cellulose,<sup>35</sup> switch-grass cellulose,<sup>36</sup> cellulose nanofiber,<sup>37</sup> and carboxymethyl cellulose.<sup>38</sup> However, films derived from a single biopolymer often exhibit suboptimal functional properties, such as poor mechanical strength or barrier performance. Thus, blending two or more biopolymers has been shown to enhance key attributes, including tensile strength, water-vapor and gas-barrier properties, UV-blocking capacity, and antioxidant activity. The present study focuses on developing biodegradable films using cellulose extract from alfalfa residue and carrageenan. Using alfalfa residue, a readily available agricultural byproduct, as a cellulose source offers a sustainable, low-cost approach to eco-friendly packaging. Alfalfa-derived cellulose films were prepared and characterized,<sup>39</sup> and carrageenan was subsequently incorporated to further enhance the films' mechanical, UV-shielding, and antioxidant properties. Carrageenan, a water-soluble natural polysaccharide extracted from red seaweed, is widely recognized for its excellent film-forming, thickening, and gelling capabilities.<sup>40,41</sup> It is abundant, renewable, biocompatible, and does not compete with agricultural land used for food production.<sup>42</sup> Owing to these advantages, carrageenan can be studied in packaging applications, particularly in combination with other biopolymers to improve film performance.<sup>41,43–45</sup> However, only a limited number of studies have examined the use of iota- and kappa-carrageenan for developing films,<sup>46–48</sup> and lambda-carrageenan has received even less attention. Thus, cellulose-carrageenan composite films would improve film properties, expanding their applications beyond their individual use.

In this study, three types of carrageenans—iota ( $\iota$ ), kappa ( $\kappa$ ), and lambda ( $\lambda$ )—were blended with alfalfa-derived cellulose to develop composite biodegradable films. The novelty lies in complexing three carrageenan types with the cellulosic residue extracted from alfalfa biomass and comparing the impacts of the  $\iota$ -,  $\kappa$ -, and  $\lambda$ -carrageenans on the film properties. It was hypothesized that the incorporation of carrageenans would enhance the films' (1) mechanical strength, (2) water vapor barrier properties, and (3) UV-blocking efficiency. Alfalfa cellulosic residue was solubilized in a zinc chloride solution, combined with predetermined amounts of carrageenan, and subsequently crosslinked using calcium chloride in the presence of the plasticizer sorbitol to form flexible films. The resulting composite films were then examined to assess their structural, mechanical, and functional properties. Overall, this

study presents a novel, sustainable strategy for using alfalfa residue as a cellulosic source and carrageenans as a natural reinforcing agent to produce biodegradable packaging films. The outcome helps reduce global plastic pollution, promotes the circular bioeconomy, and offers potential economic advantages to agricultural producers.

## 2. Materials and methods

### 2.1. Materials

Alfalfa field residue was collected from a farm in Watertown, South Dakota. The chemicals (zinc chloride, calcium chloride, sorbitol, calcium sulfate, potassium sulfate, and DPPH) were purchased from VWR International. Absolute ethanol was from the Department of Chemistry, Biochemistry, and Physics at South Dakota State University. The iota ( $\iota$ )-carrageenan (RE-PR-4018) and kappa ( $\kappa$ )-carrageenan (G1375-146-1) were gifts from FMC Biopolymer, and the lambda ( $\lambda$ )-carrageenan (P0311-3) was a gift from Shemberg Marketing Corporation.

### 2.2. Film preparation and characterization

Alfalfa cellulosic residue (ACR) extracted using alkaline and bleaching treatment, and the optimized film combination using Box-Behnken design was used from our previous study.<sup>39</sup> The optimized film combination had 0.5 g ACR, CaCl<sub>2</sub> 461.3 mM, and 1.05% sorbitol with a tensile strength of  $16.9 \pm 0.4$  MPa, elongation at break of  $10.1 \pm 0.3\%$ , and water vapor permeability of  $4.7 \pm 1.1 \times 10^{-11} \text{ g m}^{-1} \text{ s}^{-1} \text{ Pa}^{-1}$ . A slight modification was made during film preparation in a film-making solution to complex  $\iota$ -,  $\kappa$ -, and  $\lambda$ -carrageenan. Briefly, solutions of 0.5%, 1.0%, and 1.5% carrageenan were prepared separately by stirring at 300 rpm for 3 hours. The carrageenan concentration was set at an upper limit of 1.5% based on preliminary film-preparation trials, as higher concentrations were not workable for complexing and film formation due to the thicker film solution. For film preparation, 0.5 g ACR was swelled with 1.6 mL of distilled water in a water bath at 83 °C for 2 hours. A 68% ZnCl<sub>2</sub> solution was used to solubilize the ACR. After 25 min, 0.5 mL of the pre-prepared carrageenan solution was added to the solution for complexing. Later, after 5 minutes, 461.3 mM CaCl<sub>2</sub> was added and mixed for 10 minutes, followed by 1.05% sorbitol for 5 minutes. The solution was cast to form the film using a handheld applicator, then regenerated with ethanol, framed, washed, and dried at room temperature (22 °C) with a relative humidity of 47% for 24 hours. The dried film was collected and stored in an airtight container for characterization. The experimental conditions were kept constant across all film combinations. The resulting films were 0.03–0.05 mm thick. The overview of the experiment is illustrated in Fig. 1.

Films were characterized for their tensile strength, elongation at break, water vapor permeability, color, transparency, electromagnetic light transmittance, FTIR, moisture, water solubility, water contact angle, water absorption and kinetics, antioxidant activity, and soil biodegradation using established protocol.<sup>39</sup> Briefly, tensile strength and elongation at break were



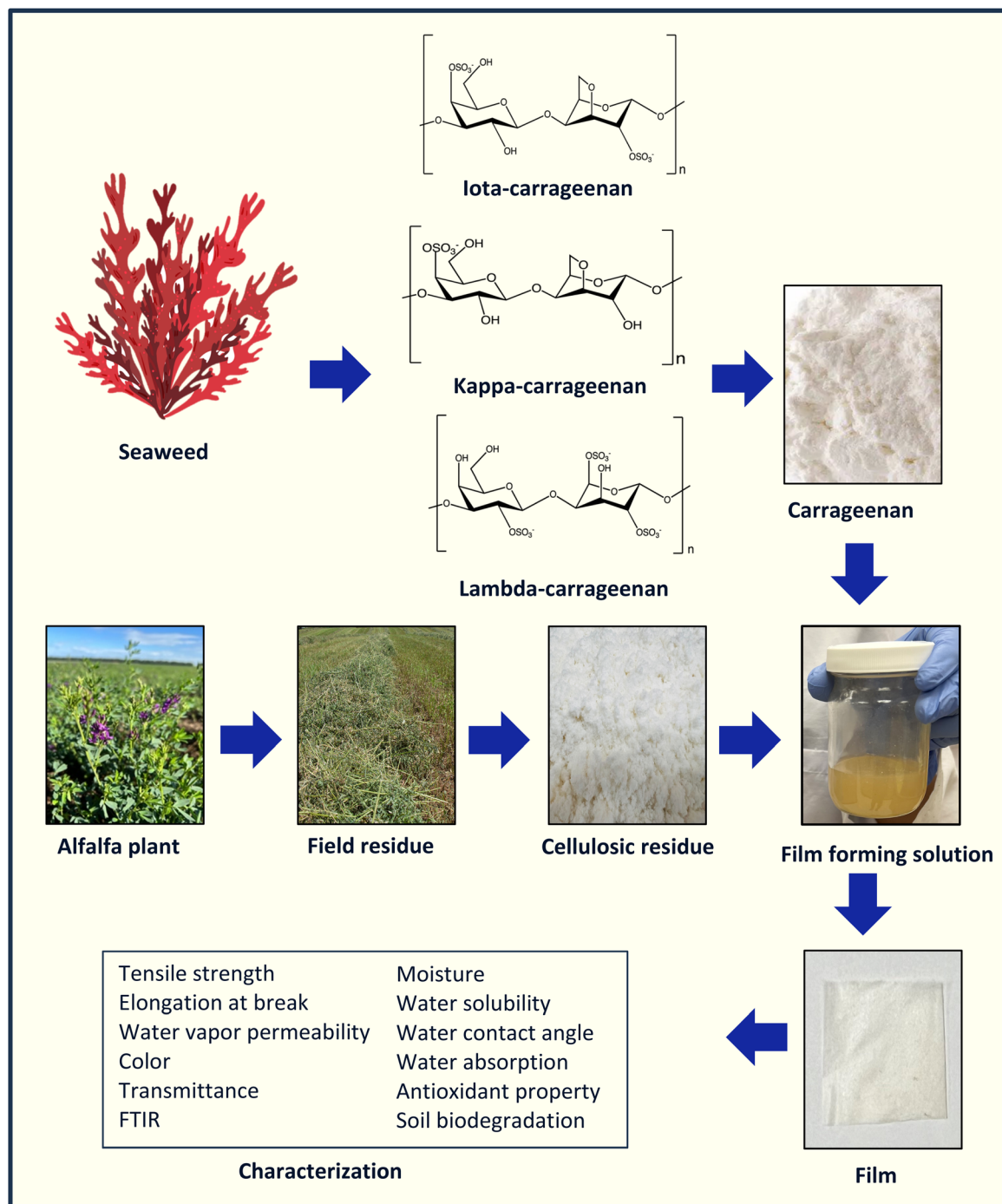


Fig. 1 The cellulosic residue from alfalfa field residue and its optimized film combination was complexed with iota-, kappa-, and lambda-carrageenan to enhance film properties. The film was characterized to understand the effect of carrageenan on various film properties.

measured using a Texture Analyzer (Stable Micro Systems, Model TA-HD plus, serial no: 5529). For water vapor permeability (WVP), a jar maintained at ~0% relative humidity (RH) with anhydrous  $\text{CaSO}_4$  was covered with film and placed in a desiccator at ~97% RH using saturated  $\text{K}_2\text{SO}_4$  solution. The weight was recorded over 8 hours, and the WVP was calculated. Color was measured in the Hunter scale using a Nix Pro 2 color sensor against a standard white background. Film transparency

was assessed using a UV-Vis spectrophotometer at 600 nm, and transmittance was measured across the 190–1060 nm range in the UV-Vis-IR region. FTIR spectra were recorded over 400–4000  $\text{cm}^{-1}$  with 36 scans at a resolution of 4  $\text{cm}^{-1}$ . Moisture content, water solubility, water absorption, and soil biodegradation were determined gravimetrically. Films were dried at 110 °C for 24 hours to determine their moisture content. Dried films were immersed in water, shaken at 175 rpm for 24 hours,



then dried again for 24 hours to assess water solubility. For water absorption, dried films were immersed in water, and their weight was recorded at 5, 10, 15, 30, 60, 90, and 120 minutes. Water absorption kinetics were analyzed using nine established models, including Peleg, Singh, Gornicki, Pilosof, Czel and Czigany, Peppas, Vega-Galvez, Garcia-Pascual, and Weibull. Films were buried in soil maintained at 24% moisture, and weight loss was recorded every other day until approximately 90% of each film was degraded. Degradation kinetics were studied with first- and second-order models. The water contact angle was measured using a dropometer by placing a water droplet and recording the resulting angle. Antioxidant activity was determined using the standard DPPH method, and  $IC_{50}$  values were calculated. All equations used for calculations are provided in the SI.

### 2.3. Statistical analysis

The composite films' properties were compared with those of the optimized film (control film) using Tukey's HSD test at a 95% confidence level in RStudio (Version 2024.09.1+394). The Solver Add-ins in Microsoft Excel for Mac (Version 16.88 (24081116)) were used to fit water absorption and soil biodegradation kinetic models.

## 3. Results and discussion

### 3.1. Mechanical properties

The incorporation of carrageenan markedly enhanced the tensile strength (TS) of ACR films. The TS increased from  $16.9 \pm 0.4$  MPa in the ACR film to a maximum of  $29.9 \pm 1.5$  MPa in the ACR- $\lambda$ 1.5% film (Fig. 2a). Across all carrageenan types, TS values rose proportionally with increasing carrageenan content. Specifically,  $\kappa$ -carrageenan films exhibited an increase to  $23.9 \pm 0.7$  MPa, while  $\iota$ -carrageenan films reached  $25.5 \pm 1.0$  MPa. The improvement in tensile strength can be attributed to electrostatic interactions and hydrogen bonding within the film matrix.<sup>49</sup> Carrageenan's sulfate groups, bearing negative charges, interact with  $Ca^{2+}$  ions to achieve charge neutralization, inducing conformational transitions that strengthen the intermolecular network.<sup>50–55</sup> Moreover, the abundant hydroxyl groups on the carrageenan chains form hydrogen bonds with cellulosic chains, further reinforcing the polymer matrix and enhancing the mechanical integrity of the films.<sup>56–60</sup> Typically,  $\kappa$ -carrageenan forms the strongest gels, followed by  $\iota$ -carrageenan. However, in the presence of calcium salts,  $\iota$ -carrageenan forms relatively strong gels, and  $\kappa$ -carrageenan tends to produce brittle gels.<sup>61–63</sup> In contrast,  $\lambda$ -carrageenan prefers viscous solutions. The uniform dispersion likely acted as a reinforcing filler in  $\lambda$ -carrageenan-containing ACR films, contributing to their superior TS. The brittleness of  $\kappa$ -carrageenan gels might be responsible for the comparatively lower TS values. Notably, the TS values of ACR-carrageenan films exceeded those reported for pure  $\iota$ -carrageenan (2.5 MPa),<sup>46</sup>  $\kappa$ -carrageenan (11.4 MPa),<sup>46</sup> cow dung cellulose (4.2 MPa),<sup>34</sup> corn cob cellulose (4.7 MPa),<sup>32</sup> soyhull cellulose (6.3 MPa),<sup>33</sup> and grapevine cellulose (18.2 MPa),<sup>35</sup> films demonstrating the superior

mechanical performance of the developed composite films. Some of the comparable films' TS are listed in Table 1.

Conversely, the elongation at break (EB) of the films significantly decreased from  $10.1 \pm 0.3\%$  for the ACR films<sup>39</sup> to as low as  $4.2 \pm 0.3\%$  for the ACR- $\iota$ 0.5% films (Fig. 2b). In the ACR- $\iota$  and ACR- $\kappa$  systems, an initial reduction in EB was observed at 0.5% carrageenan concentration, followed by a slight, statistically insignificant increase at 1% and 1.5% carrageenan amount. This minor improvement may be attributed to carrageenans gel-forming ability,<sup>61–63</sup> which can impart limited elasticity to the polymer network. In contrast, ACR- $\lambda$  films exhibited a continuous decline in EB with increasing  $\lambda$ -carrageenan content. Similar to the observed increase in tensile strength (TS), the uniform dispersion and filler effect of  $\lambda$ -carrageenan likely contributed to a denser, more rigid matrix, thereby reducing film flexibility. The EB values of the ACR-carrageenan films were higher than those of pure  $\iota$ - and  $\kappa$ -carrageenan films<sup>46</sup> and comparable to those reported for cellulose,<sup>31</sup> grapevine cellulose,<sup>35</sup> cow dung cellulose,<sup>34</sup> cellulose acetate,<sup>64</sup> soyhull lignocellulose,<sup>65,66</sup> and spent coffee ground<sup>67</sup> films. The simultaneous improvement in both TS and EB compared to pure carrageenan films highlights the synergistic interaction between alfalfa cellulosic residue and carrageenans, demonstrating the potential of these composite films for wider applications in sustainable packaging materials. A comparison of EB values for similar films is in Table 1.

### 3.2. Water vapor permeability and water interaction properties

The water vapor permeability (WVP) of the films was only slightly affected by carrageenan addition, with no statistically significant differences among the formulations. Overall, a slight decrease in WVP was noted with increasing carrageenan concentration. The WVP values ranged from  $4.3 \pm 0.3 \times 10^{-11}$  g  $m^{-1}$   $s^{-1}$   $Pa^{-1}$  for the ACR- $\kappa$  1.5% film to  $5.1 \pm 0.3 \times 10^{-11}$  g  $m^{-1}$   $s^{-1}$   $Pa^{-1}$  for the ACR- $\lambda$ 0.5% film (Fig. 2c). Carrageenans are water-soluble polysaccharides whose hydrophilic and hydrophobic behavior depends on the amount of sulfate and hydroxyl groups, as well as 3,6-anhydrogalactose units within their chain.<sup>72</sup> Sulfate groups contribute to hydrophilicity, whereas 3,6-anhydrogalactose units are linked to hydrophobicity.<sup>73,74</sup> Among the three carrageenans,  $\kappa$ -carrageenan contains the fewest of one sulfate group, followed by two in  $\iota$ - and three in  $\lambda$ -carrageenan. Consequently, ACR- $\kappa$  films exhibited lower WVP values due to their relatively hydrophobic nature, whereas ACR- $\lambda$  films showed higher WVP values reflecting their greater hydrophilicity. The WVP of ACR-carrageenan composite films was comparable to that of soyhull films<sup>65,66</sup> and switchgrass lignocellulose films,<sup>36,71</sup> and was significantly improved compared to pure  $\kappa$ - and  $\iota$ -carrageenan films<sup>46</sup> (Table 1). These results suggest that blending carrageenan with cellulose produces a well-balanced matrix with desirable film barrier properties, making it a promising material for sustainable packaging applications.

The film had a moisture content of  $10.0 \pm 0.9\%$  to  $10.8 \pm 0.9\%$  (Table 2). The carrageenan amount and type have not



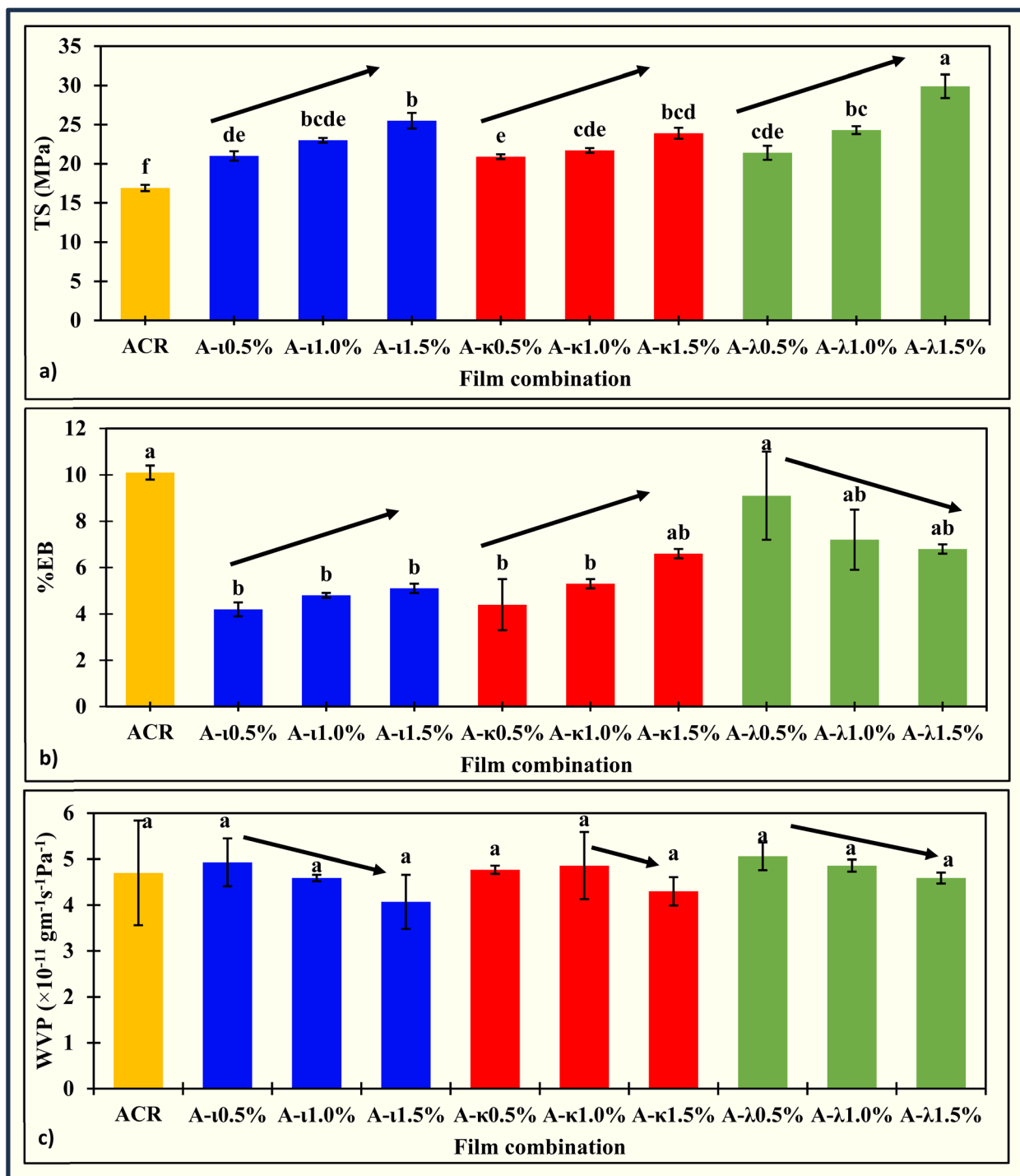


Fig. 2 Film's (a) tensile strength (TS, MPa), (b) elongation at break (EB, %), and (c) water vapor permeability (WVP,  $\times 10^{-11} \text{ g m}^{-1} \text{ s}^{-1} \text{ Pa}^{-1}$ ). The films are represented as ACR: alfalfa cellulosic residue; A-ι0.5%: ACR complexed with 0.5% iota-carrageenan, and so on, denoted κ for kappa-carrageenan and λ for lambda-carrageenan. The addition of carrageenan has improved the TS and WVP of ACR films, while EB has been reduced. The yellow, blue, red, and green color bars represent ACR, ACR-ι, ACR-κ, and ACR-λ carrageenan films, respectively. The error bars indicate the standard deviation, and the letters denote the statistical groupings from Tukey's HSD test at a 95% confidence level. The same letter suggests no significant difference, while 'a' signifies the higher value in the ascending order.

contributed to moisture retention in the films. The 24 hour film-drying process at room temperature has removed almost the same amount of moisture from the films. Likewise, the water solubility ranged from  $9.2 \pm 0.2\%$  to  $20.1 \pm 1.5\%$  (Table 2).

Interestingly, water solubility has increased significantly with increasing carrageenan concentration in the film due to carrageenan's hydrophilic nature.<sup>75</sup> Comparably, ACR-λ film showed a higher water solubility due to the viscous nature of λ-



**Table 1** Comparison of tensile strength (TS in MPa), elongation at break (EB in %), and water vapor permeability (WVP in  $10^{-11} \text{ g m}^{-1} \text{ s}^{-1} \text{ Pa}^{-1}$ ) of some films

Film	TS	EB	WVP	Reference
Alfalfa cellulose (ACR)	16.9	10.1	4.7	39
Alfalfa lignocellulose	11.2	5.8	12	68
ACR- $\iota$ -carrageenan	21.0–25.5	4.2–5.1	4.1–4.9	This work
ACR- $\kappa$ -carrageenan	20.9–23.9	4.4–6.6	4.3–4.9	This work
ACR- $\lambda$ -carrageenan	21.4–29.9	6.8–9.1	4.6–5.1	This work
$\iota$ -Carrageenan	2.5	1.0	36.1	46
$\kappa$ -Carrageenan	11.4	2.3	19.4	46
Corncob cellulose	4.7	15.4	18.0	32
Grapevine cellulose	15.4–18.2	8.6–6.1	7.0–14.0	35
Oat straw fiber	4.2–17.2	5.8–8.3	5.0–7.0	69
Sawdust lignocellulose	50.0–68.8	14.0–30.0	13.0–19.0	70
Soyhull cellulose	6.3	30.2	9.0	33
Soyhull lignocellulose	9.3	8.8	3.0	66
Soyhull lignocellulose extract	16.8	14.7	2.0	65
Spent coffee grounds lignocellulose	8.4–26.8	3.8–7.9	8.0–18.0	67
Switchgrass lignocellulose	9.9–14.7	3.4–4.7	1.0–2.0	36
Switchgrass lignocellulose extract	8.9–12.7	2.2–2.4	2.0–3.0	71

carrageenan's compared to  $\iota$ - and  $\kappa$ -carrageenan's ability to form gels.<sup>76</sup> The moisture and water solubility properties indicate that the film is suitable for packaging fresh fruits and vegetables. The moisture content and water solubility of ACR-carrageenan film closely match those of the films from grapevine cellulose,<sup>35</sup> avocado peel fiber,<sup>77</sup> wheat straw fiber,<sup>78</sup> oat straw fiber,<sup>69</sup> and soyhull lignocellulose.<sup>65,66</sup>

The water contact angle (WCA) of the films decreased from  $74.7 \pm 0.4^\circ$  to  $60.9 \pm 0.1^\circ$  (Table 2) after carrageenan addition. The WCA was significantly reduced with the presence of carrageenan, and the ACR- $\lambda$ 1.5% film had the lowest value. This indicates increased hydrophilicity of the films, due to carrageenan's hydrophilic nature.<sup>75</sup> The films tend to absorb water because of the sulfate and hydroxyl groups in the carrageenan chains.<sup>72</sup> The WCA is similar to that of  $\kappa$ -carrageenan/PVA,<sup>79</sup> chitosan-carrageenan,<sup>80</sup> corn cob cellulose,<sup>32</sup> and soyhull lignocellulose<sup>65,66</sup> films. However, further research is needed to improve the hydrophobicity of the films and expand their use on dried surface products.

Water absorption (WA) in the film results from its wettability. The hydrophilic nature of carrageenan enhances the

water absorption of the ACR films. For instance, the WA of the ACR film was  $152.0 \pm 0.2\%$  at 120 minutes, while those of A- $\iota$ 1.5%, A- $\kappa$ 1.5%, and A- $\lambda$ 1.5% were  $160.5 \pm 0.4\%$ ,  $165.1 \pm 1.5\%$ , and  $173.8 \pm 0.9\%$ , respectively (Table 2 and Fig. 3). The water absorption has greatly increased because of the higher number of hydroxyl groups in the films. The hydroxyl groups are occupied within a short period, reducing the free hydroxyl groups,<sup>81</sup> resulting in an initial higher WA that decreased over time. A similar water absorption was observed in cellulose<sup>31</sup> and banana peel fiber<sup>82</sup> films. Additionally, the water-absorption kinetics were examined using 9 established models. The coefficient of determination ( $R^2$ ) and root mean square error (RMSE) values were calculated to determine the best-fit model. The Peleg model has the highest  $R^2$  and the lowest RMSE values, ranging from 0.9997 to 0.9999 and from 0.0017 to 0.0042 (Table S1). The models Singh, Pilosof, Gornicki, Vega-Galvez, Peppas, and Czel and Czigan also met the criteria for a good fit. Gracia-Pascual and Weibull's  $R^2$  and RMSE were not detected. In the Peleg model,  $K_1$  and  $K_2$  represent the initial and maximum water-absorption capacities of the films, respectively. The  $K_1$  values ranged from 0.0056 to 0.0098, indicating an initial

**Table 2** Comparison of ACR-carrageenan film's moisture content (MC, %), water solubility (WS, %), WCA (water contact angle, °), radical scavenging activity (RSA, %) at the concentration of  $0.03 \text{ g mL}^{-1}$ , and  $\text{IC}_{50}$  values. The letters in the superscript indicate the statistical groups from Tukey's HSD test at a 95% confidence level, with the same letter signifying no significant difference, arranged in ascending order, where 'a' represents the higher value following ascending order

Film	MC	WS	WCA	WA <sub>120</sub>	RSA	IC <sub>50</sub>
ACR	$10.0 \pm 0.9^a$	$9.2 \pm 0.2^c$	$74.7 \pm 0.4^a$	$152.0 \pm 0.2^c$	$7.32 \pm 0.08^c$	$0.41 \pm 0.01^a$
ACR- $\iota$ 0.5%	$10.8 \pm 0.4^a$	$13.2 \pm 1.1^b$	$66.0 \pm 0.9^d$	$156.1 \pm 0.1^d$	$9.53 \pm 0.09^a$	$0.41 \pm 0.03^a$
ACR- $\iota$ 1.0%	$10.0 \pm 0.3^a$	$14.5 \pm 0.9^b$	$62.7 \pm 0.2^{ef}$	$160.0 \pm 0.4^c$	$9.36 \pm 0.01^{ab}$	$0.40 \pm 0.01^a$
ACR- $\iota$ 1.5%	$10.4 \pm 0.3^a$	$16.5 \pm 1.4^{ab}$	$62.2 \pm 0.4^{ef}$	$160.5 \pm 0.4^c$	$9.58 \pm 0.15^a$	$0.38 \pm 0.01^a$
ACR- $\kappa$ 0.5%	$10.5 \pm 0.6^a$	$13.8 \pm 0.2^b$	$69.2 \pm 1.6^{bc}$	$155.6 \pm 0.9^{de}$	$8.86 \pm 0.07^b$	$0.41 \pm 0.02^a$
ACR- $\kappa$ 1.0%	$10.2 \pm 0.1^a$	$15.3 \pm 1.5^b$	$66.2 \pm 0.5^{cd}$	$156.8 \pm 0.5^{cd}$	$9.14 \pm 0.01^{ab}$	$0.40 \pm 0.02^a$
ACR- $\kappa$ 1.5%	$10.8 \pm 0.9^a$	$17.0 \pm 0.7^{ab}$	$62.0 \pm 0.7^{ef}$	$165.1 \pm 1.5^b$	$9.42 \pm 0.07^{ab}$	$0.39 \pm 0.02^a$
ACR- $\lambda$ 0.5%	$10.7 \pm 0.4^a$	$14.2 \pm 0.1^b$	$70.5 \pm 0.4^b$	$160.3 \pm 1.8^c$	$9.25 \pm 0.31^{ab}$	$0.41 \pm 0.03^a$
ACR- $\lambda$ 1.0%	$10.3 \pm 0.2^a$	$16.8 \pm 0.6^{ab}$	$65.0 \pm 1.2^{de}$	$167.2 \pm 1.2^b$	$9.36 \pm 0.16^{ab}$	$0.39 \pm 0.03^a$
ACR- $\lambda$ 1.5%	$10.4 \pm 1.2^a$	$20.1 \pm 1.5^a$	$60.9 \pm 0.1^f$	$173.9 \pm 0.9^a$	$9.64 \pm 0.23^a$	$0.36 \pm 0.01^a$



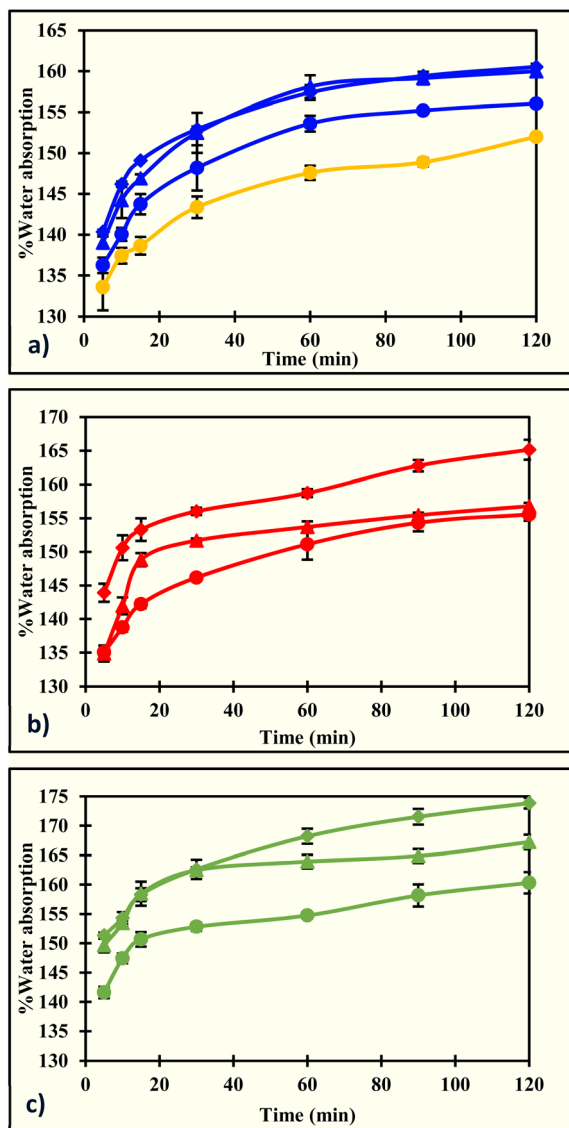


Fig. 3 The %water absorption of (a) ACR films (yellow line) and ACR-l-carrageenan films (blue lines), (b) ACR-k-carrageenan films (red lines), and (c) ACR-lambda-carrageenan films (green lines). The films ACR, ACR-l0.5%, ACR-l1.0%, ACR-l1.5%, ACR-k0.5%, ACR-k1.0%, ACR-k1.5%, ACR-lambda0.5%, ACR-lambda1.0%, and ACR-lambda1.5% are denoted by  $\square$ ,  $\circ$ ,  $\triangle$ ,  $\square$ ,  $\circ$ ,  $\triangle$ ,  $\square$ ,  $\circ$ ,  $\triangle$ ,  $\square$ ,  $\circ$ ,  $\triangle$ , and  $\square$ , respectively. The error bars indicate the standard deviation.

moisture absorption of  $133.6 \pm 2.8\%$  to  $151.3 \pm 0.5\%$ . Similarly, the  $K_2$  ranged from 0.0057 to 0.0066, showing a higher maximum water absorption capacity for the films, ranging from  $152.0 \pm 0.2\%$  to  $173.9 \pm 0.9\%$ . The films made from agar,<sup>83</sup> grapevine cellulose,<sup>35</sup> cellulose/ulvan composite,<sup>84</sup> corncob cellulose,<sup>32</sup> cow dung cellulose,<sup>34</sup> soyhull cellulose,<sup>33</sup> soyhull lignocellulose,<sup>65,66</sup> switchgrass lignocellulose,<sup>36,71</sup> alfalfa lignocellulose,<sup>68</sup> and spent coffee grounds<sup>67</sup> exhibited similar  $K_1$  and  $K_2$  values and followed Peleg water absorption kinetics.

### 3.3. Color

The film's color, an important aesthetic feature, changed subtly. Values for  $L^*$ ,  $a^*$ ,  $b^*$ , whiteness index (WI), yellowness index

(YI), and total color difference (TCD) ranged from  $83.7 \pm 0.6$  to  $87.3 \pm 0.9$ ,  $0.5 \pm 0.5$  to  $1.4 \pm 0.6$ ,  $6.5 \pm 0.4$  to  $9.2 \pm 0.7$ ,  $81.3 \pm 0.6$  to  $85.6 \pm 0.8$ ,  $10.7 \pm 0.6$  to  $15.7 \pm 1.0$ , and  $6.8 \pm 0.3$  to  $10.9 \pm 0.4$ , respectively (Table 3). Significant changes were observed in  $L^*$ ,  $b^*$ , WI, YI, and TCD, indicating decreased lightness, a more pronounced yellow hue, lower whiteness, increased yellowness, and a greater deviation from the standard white background. Although the  $a^*$  values increased slightly—implying a minor shift toward red—this change was not significant. Since carrageenan naturally ranges from yellowish to white,<sup>85</sup> these slight color shifts are expected. The observed values are consistent with those reported for films made from grapevine,<sup>35</sup> banana peel fiber,<sup>79</sup> corncob,<sup>32</sup> cow dung,<sup>34</sup> and soy hull cellulose.<sup>33</sup>

### 3.4. Transparency and transmittance of electromagnetic radiation

The film's transparency slightly decreased with the addition of carrageenan. The reduction was statistically significant, dropping from  $27.3 \pm 0.6 \text{ \%mm}^{-1}$  in ACR film to  $25.7 \pm 0.1 \text{ \%mm}^{-1}$ , and to  $24.6 \pm 0.5 \text{ \%mm}^{-1}$  and  $25.4 \pm 0.3 \text{ \%mm}^{-1}$  in ACR-l1.5%, ACR-k1.5%, and ACR-lambda1.5% films, respectively (Table 3).

The transmittance of electromagnetic radiation was examined for the films with the lowest transparency in each carrageenan category, namely, the ACR-l1.5%, ACR-k1.5%, and ACR-lambda1.5% films. In the UVC region at 190 nm, the light transmittance was  $45.5 \pm 0.9\%$ ,  $35.4 \pm 0.6\%$ ,  $38.9 \pm 0.3\%$ , and  $25.7 \pm 0.8\%$  in the ACR, ACR-l1.5%, ACR-k1.5%, and ACR-lambda1.5% films, respectively (Fig. 4a), and gradually increased to  $62.0 \pm 0.1\%$ ,  $53.9 \pm 0.4\%$ ,  $55.3 \pm 0.8\%$ , and  $47.5 \pm 0.4\%$  at 260 nm. Furthermore, transmittance steadily decreased to  $9.2 \pm 0.4\%$ ,  $5.2 \pm 0.6\%$ ,  $6.5 \pm 0.8\%$ , and  $7.0 \pm 0.4\%$  at 310 nm in the UVB region, with a slight increase in the UVA region reaching  $17.7 \pm 1.1\%$ ,  $15.6 \pm 1.2\%$ ,  $14.3 \pm 0.1\%$ , and  $15.5 \pm 0.5\%$  at 390 nm. The slight elevation continued through the visible and IR regions, with values of  $23.1 \pm 1.1\%$ ,  $16.9 \pm 0.1\%$ ,  $19.0 \pm 0.6\%$ , and  $19.4 \pm 0.6\%$  at 700 nm, and  $25.4 \pm 1.8\%$ ,  $17.7 \pm 0.1\%$ ,  $20.4 \pm 1.0\%$ , and  $21.4 \pm 1.1\%$  at 1060 nm, respectively. Overall, the presence of carrageenan has improved light-blocking properties compared to those of the ACR film, with the highest blockage observed with the ACR-l1.5% film. The ACR-carrageenan film's light-blocking ability is comparable to that of the spent coffee grounds<sup>67</sup> and corncob cellulose<sup>32</sup> films and better than soyhull cellulose,<sup>33</sup> and lignocellulose,<sup>65,66</sup> and cow dung cellulose<sup>34</sup> films. This property helps slow photodegradation and protect food products, such as fruits and vegetables, from vitamin and pigment loss, as well as dairy, meat, and fish products from discoloration and rancidity.<sup>86</sup>

Additionally, the film's absorption coefficient was calculated across the UV-Vis-IR region (Fig. 4b). The absorption coefficients of the ACR, ACR-l1.5%, ACR-k1.5%, and ACR-lambda1.5% films were  $15.8 \pm 0.4$ ,  $20.8 \pm 0.4$ ,  $18.9 \pm 0.2$ , and  $27.2 \pm 0.6$  at 190 nm, decreasing to  $9.6 \pm 0.1$ ,  $12.4 \pm 0.1$ ,  $11.9 \pm 0.3$ , and  $14.9 \pm 0.2$  at 260 nm in the UVC region, respectively. The absorption coefficient increased to  $47.8 \pm 0.9$ ,  $59.2 \pm 2.1$ ,  $54.8 \pm 2.4$ , and  $53.1 \pm 1.2$  at 310 nm in the UVB region. There was a slight decrease in



**Table 3** Film's color in Hunter scale  $L^*$ ,  $a^*$ ,  $b^*$ , whiteness index (WI), yellowness index (YI), and total color difference (TCD), and film's transparency (Trans, %mm<sup>-1</sup>). The superscript letters identify the Tukey's HSD groupings at a 95% confidence level. Values assigned the same letter do not differ significantly. The letters are assigned in ascending order, with 'a' representing the highest value within each grouping

Film	$L^*$	$a^*$	$b^*$	WI	YI	TCD	Trans
ACR	87.3 ± 0.9 <sup>a</sup>	0.7 ± 0.2 <sup>a</sup>	6.6 ± 0.3 <sup>c</sup>	85.6 ± 0.8 <sup>a</sup>	10.8 ± 0.5 <sup>c</sup>	6.8 ± 0.3 <sup>f</sup>	27.3 ± 0.6 <sup>a</sup>
ACR- $\iota$ 0.5%	86.9 ± 0.3 <sup>a</sup>	0.5 ± 0.5 <sup>a</sup>	8.1 ± 0.7 <sup>ab</sup>	84.6 ± 0.3 <sup>ab</sup>	13.2 ± 1.1 <sup>b</sup>	8.3 ± 0.5 <sup>de</sup>	26.8 ± 0.2 <sup>ab</sup>
ACR- $\iota$ 1.0%	84.3 ± 0.4 <sup>cd</sup>	0.6 ± 0.6 <sup>a</sup>	8.2 ± 0.7 <sup>ab</sup>	82.3 ± 0.6 <sup>c</sup>	13.8 ± 1.2 <sup>ab</sup>	9.7 ± 0.7 <sup>bc</sup>	26.4 ± 0.1 <sup>abc</sup>
ACR- $\iota$ 1.5%	84.1 ± 1.0 <sup>cd</sup>	0.7 ± 0.4 <sup>a</sup>	8.2 ± 0.5 <sup>ab</sup>	82.1 ± 1.0 <sup>c</sup>	13.9 ± 0.9 <sup>ab</sup>	9.8 ± 0.8 <sup>abc</sup>	25.7 ± 0.1 <sup>bed</sup>
ACR- $\kappa$ 0.5%	85.4 ± 1.0 <sup>bc</sup>	0.8 ± 0.4 <sup>a</sup>	6.6 ± 0.7 <sup>c</sup>	83.9 ± 1.1 <sup>b</sup>	11.1 ± 1.2 <sup>c</sup>	7.8 ± 1.0 <sup>ef</sup>	26.1 ± 0.2 <sup>abc</sup>
ACR- $\kappa$ 1.0%	84.1 ± 0.3 <sup>cd</sup>	1.4 ± 0.3 <sup>a</sup>	7.4 ± 0.9 <sup>bc</sup>	82.4 ± 0.1 <sup>c</sup>	12.5 ± 1.6 <sup>bc</sup>	9.3 ± 0.5 <sup>cd</sup>	25.5 ± 0.2 <sup>cd</sup>
ACR- $\kappa$ 1.5%	83.7 ± 0.6 <sup>d</sup>	1.4 ± 0.6 <sup>a</sup>	7.4 ± 0.8 <sup>bc</sup>	82.1 ± 0.6 <sup>c</sup>	12.5 ± 1.3 <sup>bc</sup>	9.5 ± 0.7 <sup>bc</sup>	24.6 ± 0.5 <sup>d</sup>
ACR- $\lambda$ 0.5%	86.2 ± 0.7 <sup>ab</sup>	1.0 ± 0.7 <sup>a</sup>	6.5 ± 0.4 <sup>c</sup>	84.7 ± 0.6 <sup>ab</sup>	10.7 ± 0.6 <sup>c</sup>	7.3 ± 0.5 <sup>ef</sup>	27.3 ± 0.3 <sup>a</sup>
ACR- $\lambda$ 1.0%	84.2 ± 1.2 <sup>cd</sup>	1.2 ± 1.0 <sup>a</sup>	9.0 ± 0.4 <sup>ab</sup>	81.8 ± 1.0 <sup>c</sup>	15.3 ± 0.8 <sup>a</sup>	10.5 ± 0.7 <sup>ab</sup>	25.6 ± 0.2 <sup>cd</sup>
ACR- $\lambda$ 1.5%	83.8 ± 0.9 <sup>d</sup>	1.1 ± 0.6 <sup>a</sup>	9.2 ± 0.7 <sup>ab</sup>	81.3 ± 0.6 <sup>c</sup>	15.7 ± 1.0 <sup>a</sup>	10.9 ± 0.4 <sup>a</sup>	25.4 ± 0.3 <sup>cd</sup>

the UVA region, extending through the visible and IR regions, with measurements of  $34.7 \pm 1.3$ ,  $37.3 \pm 1.6$ ,  $39.0 \pm 0.1$ ,  $37.4 \pm 0.6$ ,  $29.4 \pm 0.9$ ,  $35.6 \pm 0.1$ ,  $33.3 \pm 0.7$ ,  $32.9 \pm 0.7$ , and  $27.4 \pm 1.4$ ,

$34.7 \pm 0.1$ ,  $31.8 \pm 1.0$ , and  $30.9 \pm 1.0$ , respectively. This indicates that the ACR-carrageenan films can effectively protect packaged material from UV radiation.

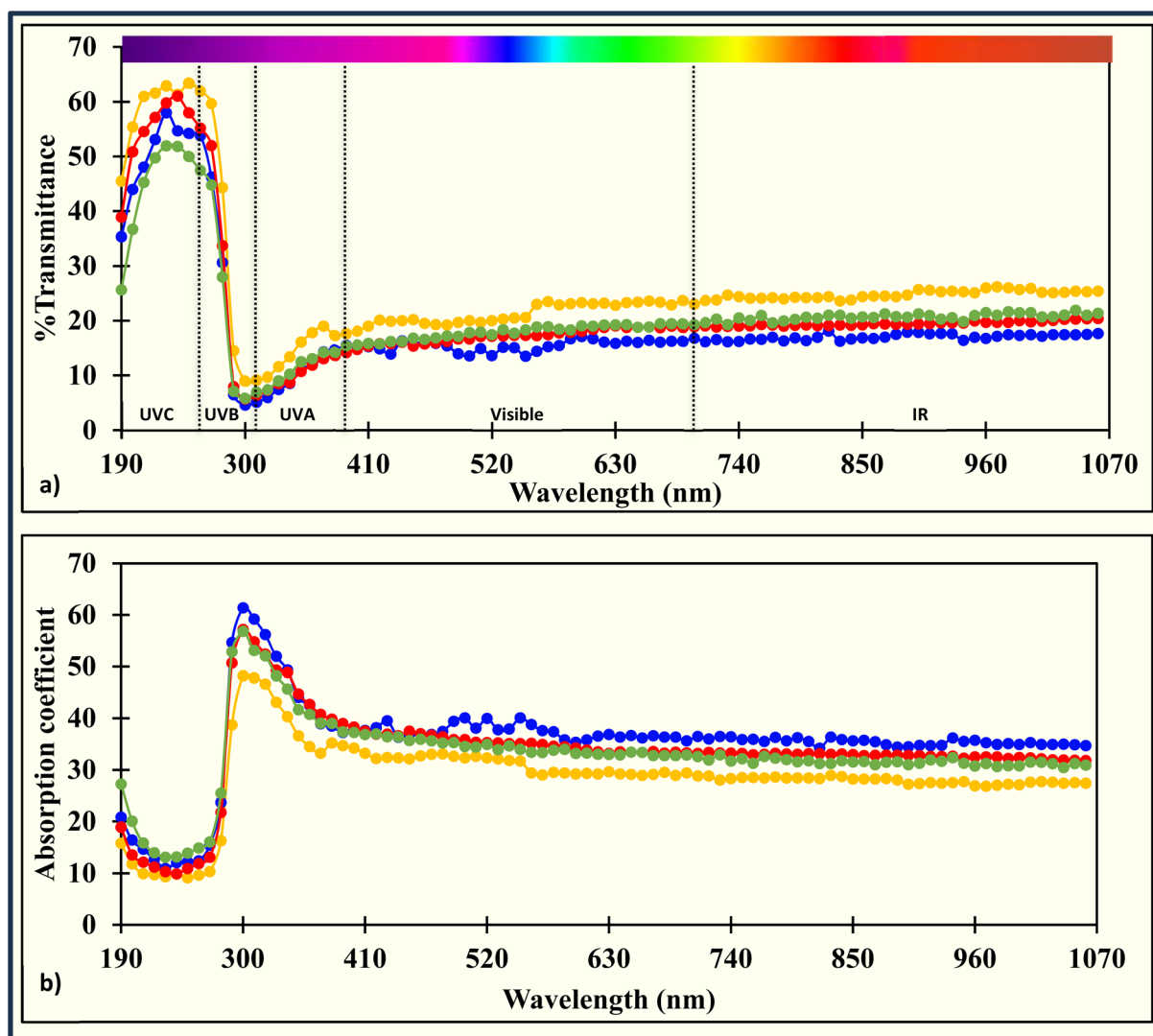


**Fig. 4** Film's (a) % transmittance and (b) absorption coefficient of the electromagnetic radiation throughout the UV-Vis-IR region. Yellow, blue, red, and green lines are given for ACR (yellow line), ACR- $\iota$ 1.5% (blue line), ACR- $\kappa$ 1.5% (red line), and ACR- $\lambda$ 1.5% (green line) films, respectively. The addition of carrageenan has significantly improved the light-blocking capability of films.



### 3.5. FTIR

During film formation, most of the FTIR peaks were either retained or shifted from the ACR film, while a few disappeared or were newly formed. The peaks listed for the ACR film were at 666, 697, 765, 897, 1023, 1156, 1205, 1271, 1318, 1326, 1371, 1424, 1616, 1734, 2857 to 2895, and 3280 to 3350  $\text{cm}^{-1}$  (ref. 39)

(Fig. S1). The peaks at 667, 766, 806, 894, 1015, 1154, 1203, 1238, 1264, 1320, 1369, 1424, 1615, 2857 to 2921, and 3280 to 3370  $\text{cm}^{-1}$  were observed in the ACR-1.5% film (Fig. 5a). Most of the peaks are either shifted or unchanged from the ACR film, indicating that the presence of cellulose, xylan, and mannan was not disturbed in the film matrix. The peak shift results from

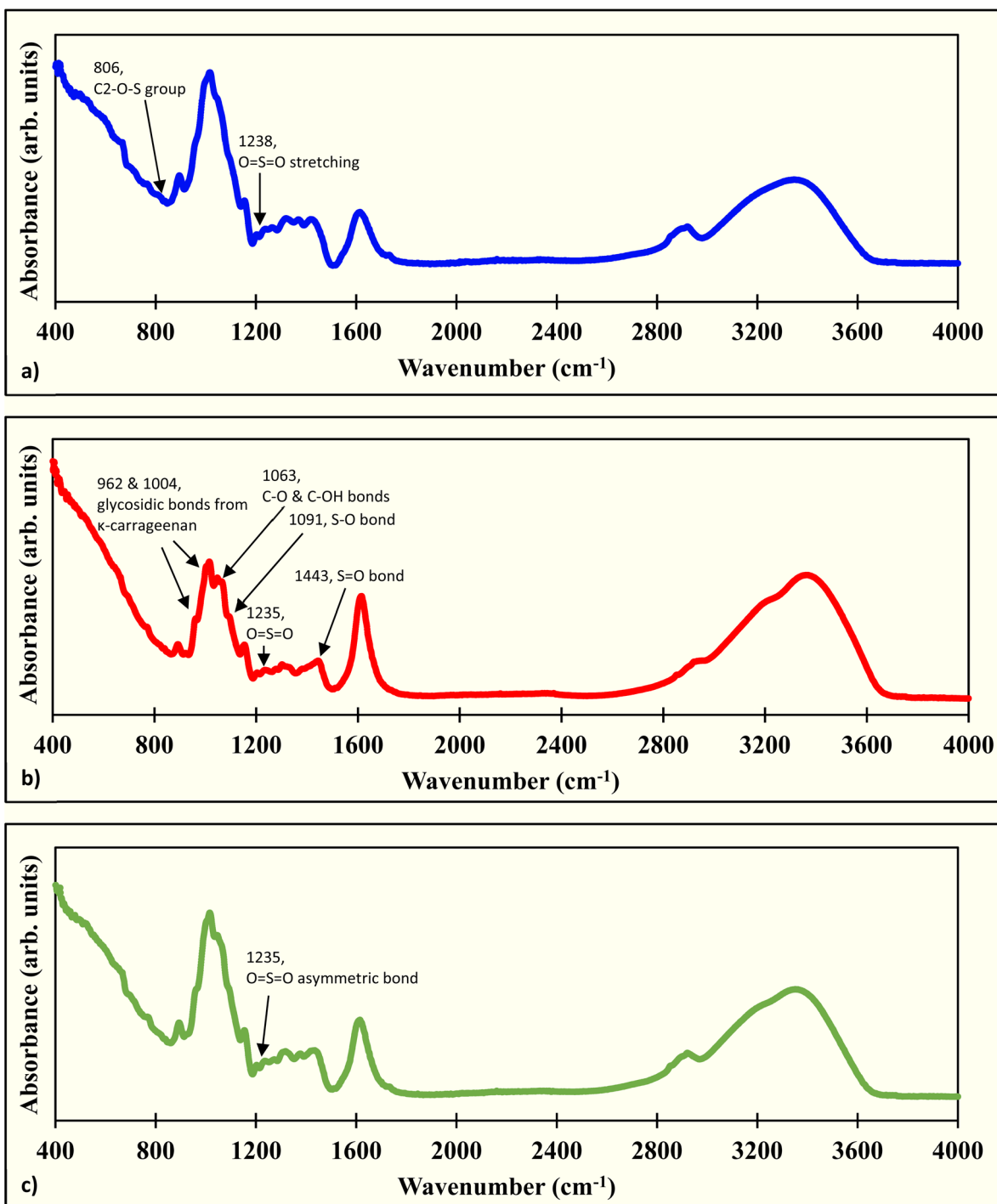


Fig. 5 FTIR spectrum of (a) ACR-1.5% (blue line), (b) ACR- $\kappa$ 1.5% (red line), and (c) ACR- $\lambda$ 1.5% (green line) film. The representative peaks are newly formed peaks caused by the addition of carrageenan to the ACR films. The detailed FTIR spectra of the alfalfa cellulosic residue (ACR) and the ACR film are provided in our previous study and shown in Fig. S1. The spectrum reveals the presence of cellulose, xylan, and mannan chains in the film system, and they remain after complexing with carrageenan.



their chemical interactions with by  $\iota$ -carrageenan in the film. Additionally, the peaks at 697, 1326, and 1734  $\text{cm}^{-1}$  disappeared in the ACR- $\iota$ 1.5% film. The peaks at 697 and 1326  $\text{cm}^{-1}$  form during film formation due to interactions among cellulosic residue, Zn ions, and Ca ions. This interaction might be influenced by  $\iota$ -carrageenan. The band at 1734  $\text{cm}^{-1}$  indicates the loss of the C=O stretching of the ketone and carbonyl groups.<sup>87</sup> The new peaks at 806 and 1238  $\text{cm}^{-1}$  could originate from  $\iota$ -carrageenan. The peak at 806  $\text{cm}^{-1}$  represents the C2-O-S group from the 3,6-anhydrogalactose-2-sulfate.<sup>88-90</sup> The band at 1238  $\text{cm}^{-1}$  is attributed to O=S=O asymmetric stretching.<sup>88-90</sup>

The peaks present in the ACR- $\kappa$ 1.5% films are at 667, 768, 892, 962, 1004, 1015, 1063, 1091, 1152, 1204, 1235, 1278, 1302, 1318, 1382, 1443, 1614, 2923, and 3280 to 3370  $\text{cm}^{-1}$  (Fig. 5b).

The 697, 1326, 1424, and 1734  $\text{cm}^{-1}$  bands have disappeared, suggesting the deformation due to the additional interaction with  $\kappa$ -carrageenan. The peak at 1424  $\text{cm}^{-1}$  indicates a deformation of one of the xylan peaks in the film matrix due to  $\kappa$ -carrageenan, but it is retained in the ACR- $\iota$ 1.5% film. The mannan peak at 2857 to 2895  $\text{cm}^{-1}$  was reduced to a 2923  $\text{cm}^{-1}$  peak. The newly formed peaks at 962, 1004, 1063, 1091, 1235, 1302, and 1443  $\text{cm}^{-1}$  are due to the  $\kappa$ -carrageenan. The peaks at 962 and 1004  $\text{cm}^{-1}$  correspond to the glycosidic bonds of  $\kappa$ -carrageenan.<sup>88,91</sup> The C-O and C-OH bonds are represented by 1063  $\text{cm}^{-1}$ ,<sup>91-93</sup> symmetric stretching of S-O bonds by 1091  $\text{cm}^{-1}$ ,<sup>92-94</sup> asymmetric stretching of O=S=O bonds by 1235  $\text{cm}^{-1}$ ,<sup>89,90,93,94</sup> and methyl group vibration due to S=O asymmetric stretch by 1443  $\text{cm}^{-1}$  peaks.<sup>95</sup> The 1302  $\text{cm}^{-1}$  band is due to a chemical interaction with  $\kappa$ -carrageenan during film

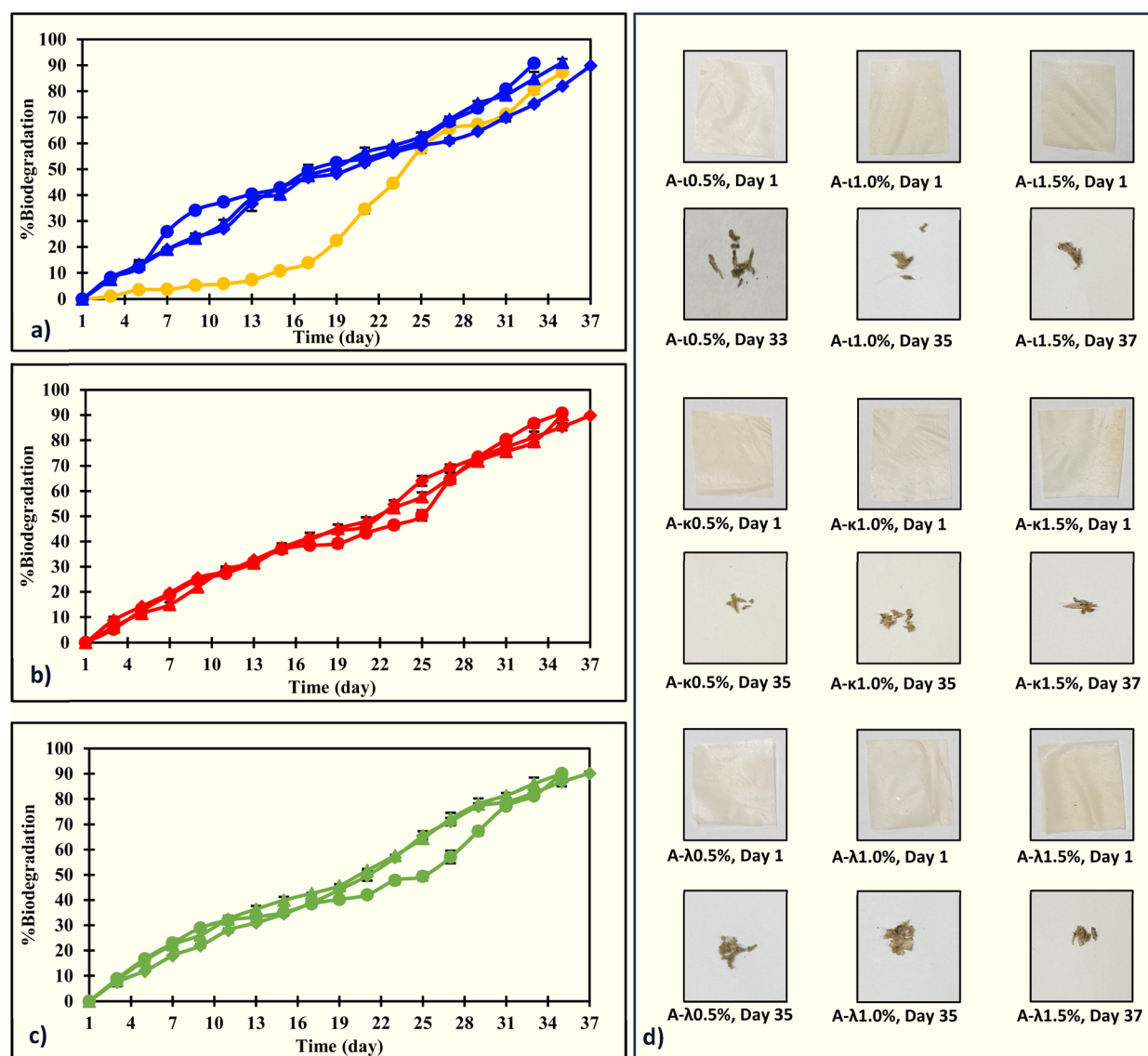


Fig. 6 The % biodegradation of the (a) ACR (yellow line) and ACR- $\iota$ -carrageenan film (blue lines), (b) ACR- $\kappa$ -carrageenan film (red lines), and (c) ACR- $\lambda$ -carrageenan film (green lines). The films ACR, A- $\iota$ 0.5%, A- $\iota$ 1.0%, A- $\iota$ 1.5%, A- $\kappa$ 0.5%, A- $\kappa$ 1.0%, A- $\kappa$ 1.5%, A- $\lambda$ 0.5%, A- $\lambda$ 1.0%, and A- $\lambda$ 1.5% are denoted by  $\circ$ ,  $\square$ ,  $\triangle$ ,  $\diamond$ ,  $\circ$ ,  $\square$ ,  $\triangle$ ,  $\diamond$ ,  $\circ$ ,  $\square$ ,  $\triangle$ , and  $\diamond$ , respectively. (d) Films before and after biodegradation. The error bars indicate the standard deviation.



formation and corresponds to the sugar backbone of the carbohydrate.

Similarly, the peaks at 666, 767, 893, 1016, 1154, 1203, 1235, 1273, 1317, 1377, 1424, 1615, 2920, and 3280 to 3370  $\text{cm}^{-1}$  were present in the ACR- $\lambda$ 1.5% film (Fig. 5c). The disappearance was similar to that observed in other carrageenan films, at 697, 1326, and 1734  $\text{cm}^{-1}$ , with the peaks around 2857 to 2895  $\text{cm}^{-1}$  shrinking toward the 2920  $\text{cm}^{-1}$  peak. There was only one new peak at 1235  $\text{cm}^{-1}$ , corresponding to the asymmetric stretching of the O=S=O bonds.<sup>86,87,90,91</sup>

The FTIR peaks indicate the presence of sulfide groups and increased hydroxyl groups in the ACR-carrageenan films, confirming the enhanced mechanical strength reported earlier in Section 3.1. Overall, interactions among cellulosic residue, carrageenan chains, and calcium ions led to peak formation, deformation, and shifting, with some peaks intensifying.

### 3.6. Antioxidant activity

The antioxidant activity of the packaging material is vital for developing active packaging. Antioxidant properties indicate the ability to neutralize free radicals. Here, a slight improvement in antioxidant activity was observed due to the presence of carrageenan in the films. The  $\lambda$ -carrageenan resulted in higher antioxidant activity with radical scavenging activity (RSA) at 0.03  $\text{g mL}^{-1}$  concentration was  $9.64 \pm 0.23\%$  and an  $\text{IC}_{50}$  value of  $0.36 \pm 0.01 \text{ g mL}^{-1}$ , followed by  $\iota$ -carrageenan,  $9.58 \pm 0.15\%$  and  $0.38 \pm 0.01 \text{ g mL}^{-1}$ , and  $\kappa$ -carrageenan,  $9.42 \pm 0.07\%$  and  $0.39 \pm 0.02 \text{ g mL}^{-1}$  (Table 2). This could be due to a higher free sulfate content in the carrageenan, in the order of  $\lambda > \iota > \kappa$ -carrageenan, which influences the free radical scavenging ability of the films.<sup>73,74,96</sup> The antioxidant activity helps extend the shelf-life of fresh fruits and vegetables and offers a step toward sustainable, active food packaging.

### 3.7. Soil biodegradation

The ACR and ACR-carrageenan films fully degraded within 40 days (Fig. 6). Overall, the initial degradation rate of the ACR-carrageenan films was faster than that of the ACR film, while the later degradation was slower. After about 21 days, the ACR film loses about one-third of its weight, while the ACR-carrageenan films lose about half. Later, the ACR film took 35 days, and the ACR-carrageenan films took 33–37 days to degrade to nearly 90% of their original size. The faster biodegradation might be due to the films' effective water interaction, facilitated by hydroxyl groups. A similar effect was reported in the carrageenan-based films.<sup>97,98</sup>

The biodegradation trend was examined using both first-order and second-order reduction reaction kinetics (Table S2). Throughout the study, all film combinations exhibited second-order reduction reaction kinetics, with  $R^2$  values ranging from 0.9146 to 0.9852 and RMSE values between 0.0854 and 0.2015. The half-lives of the ACR film, ACR- $\iota$ -carrageenan films, A- $\kappa$ -carrageenan films, and A- $\lambda$ -carrageenan films were 25.8, 17.0–19.3, 19.8–20.8, and 18.7–21.6 days, respectively. Films made from corncob cellulose,<sup>32</sup> soyhull cellulose,<sup>33</sup> soyhull

lignocellulose,<sup>65,66</sup> grapevine cellulose,<sup>35</sup> and cow dung cellulose<sup>34</sup> also followed second-order reduction kinetics.

## 4. Conclusions

Plastic pollution has become a global environmental crisis due to its durability, non-biodegradability, and widespread use in single-use items like food packaging. Conventional plastics can last for centuries in the environment, leading to large amounts of waste in landfills, terrestrial ecosystems, and oceans. Over time, these plastics break down into micro- and nano-sized particles that contaminate soil, water, and air. Microplastics have been found in rivers, oceans, and even drinking water, raising serious ecological and human health concerns. In this context, biodegradable packaging options offer a promising way to reduce plastic pollution. This study successfully developed biodegradable composite films made from alfalfa cellulosic residue reinforced with carrageenan ( $\iota$ -,  $\kappa$ -, and  $\lambda$ -carrageenan), providing a sustainable alternative to petroleum-based plastic packaging. The addition of carrageenan significantly improved the functional performance of films based on alfalfa cellulosic residue. The films exhibited a notable increase in tensile strength, supporting the first hypothesis. The reduction in water vapor permeability indicated enhanced moisture-barrier performance, thereby validating the second hypothesis. Additionally, the incorporation of carrageenan significantly improved the films' UV-blocking capacity, confirming the third hypothesis. Among the prepared films, ACR- $\lambda$ -carrageenan films showed superior performance; however, further research on their properties is needed to meet packaging needs. The enhanced antioxidant activity conferred the films multifunctional qualities, making them suitable for food packaging. The results indicate that blending complementary biopolymers rather than relying on a single polymer system effectively improves film properties. The synergistic interactions between cellulose and carrageenan enhanced mechanical strength and functional features, such as UV protection and antioxidant capacity—key factors for extending the shelf life of packaged foods. Future research should focus on developing biodegradable films from various sources of cellulosic residue combined with different biopolymers and additives. It should also explore lifecycle assessment, techno-economic analysis, packaging applications, and scale-up production for commercial purposes. Overall, this research introduces an eco-friendly, circular approach by valorizing agricultural residues, such as alfalfa as a cellulose source, and utilizing seaweed-derived carrageenan as a natural reinforcing agent. This strategy tackles the pressing challenges of plastic pollution while adding value to agricultural and marine byproducts. As a result, alfalfa cellulose-carrageenan composite films have significant potential as sustainable, non-toxic, and renewable materials for next-generation biodegradable food packaging applications.

## Author contributions

Sandeep Paudel: data curation; formal analysis; methodology; investigation; visualization; software; validation; writing—



original draft; review & editing. Srinivas Janaswamy: conceptualization; methodology; resources; writing—review & editing; supervision; project administration; funding acquisition.

## Conflicts of interest

There are no conflicts to declare.

## Data availability

Data will be made available on request.

Supplementary information (SI): equations, FTIR spectra of ACR and ACR film, and water absorption and biodegradation kinetic model fittings. See DOI: <https://doi.org/10.1039/d5fb00872g>.

## Acknowledgements

We thank the National Alfalfa & Forage Alliance, USDA Agriculture Research Service (agreement number 58-5010-3-012) and USDA National Institute of Food and Agriculture (SD00G677-20, 2021-67022-33469, and SD00H772-22) for the financial support; Dr Kasiviswanathan Muthukumarappan for access to the Texture Analyzer; Dr Todd Letcher for access to FTIR; Mr Phil Taecker for generous supply of alfalfa from his farm, and Ms Ann Taecker for help with biomass procuring and processing.

## References

- 1 Plastic Oceans, *The Facts*, <https://www.plasticoceans.org/blog/the-facts>, accessed 29 October 2025.
- 2 G. G. N. Thushari and J. D. M. Senevirathna, Plastic pollution in the marine environment, *Helvion*, 2020, **6**, e04709.
- 3 R. E. J. Schnurr, V. Alboiu, M. Chaudhary, R. A. Corbett, M. E. Quanz, K. Sankar, H. S. Srain, V. Thavarajah, D. Xanthos and T. R. Walker, Reducing marine pollution from single-use plastics (SUPs): a review, *Mar. Pollut. Bull.*, 2018, **137**, 157–171.
- 4 L. M. Heidbreder, I. Bablok, S. Drews and C. Menzel, Tackling the plastic problem: a review on perceptions, behaviors, and interventions, *Sci. Total Environ.*, 2019, **668**, 1077–1093.
- 5 C. J. Rhodes, Plastic pollution and potential solutions, *Sci. Prog.*, 2018, **101**, 207–260.
- 6 K. Taylor-Smith, *How Plastic Pollution is Affecting the Ocean Wildlife*, <https://www.azocleantech.com/article.aspx?ArticleID=729>, accessed 5 March 2025.
- 7 A. T. Williams and N. Rangel-Buitrago, The past, present, and future of plastic pollution, *Mar. Pollut. Bull.*, 2022, **176**, 113429.
- 8 P. Ayassamy, Ocean plastic pollution: a human and biodiversity loop, *Environ. Geochem. Health*, 2025, **47**, 91.
- 9 A. A. Horton, Plastic pollution: when do we know enough?, *J. Hazard. Mater.*, 2022, **422**, 126885.
- 10 D. Xanthos and T. R. Walker, International policies to reduce plastic marine pollution from single-use plastics (plastic bags and microbeads): a review, *Mar. Pollut. Bull.*, 2017, **118**, 17–26.
- 11 H. Dong, X. Wang, X. Niu, J. Zeng, Y. Zhou, Z. Suona, Y. Yuan and X. Chen, Overview of analytical methods for the determination of microplastics: current status and trends, *TrAC, Trends Anal. Chem.*, 2023, **167**, 117261.
- 12 G. Kutralam-Muniasamy, V. C. Shruti, F. Pérez-Guevara and P. D. Roy, Microplastic diagnostics in humans: “The 3Ps” progress, problems, and prospects, *Sci. Total Environ.*, 2023, **856**, 159164.
- 13 S. Matavos-Aramyan, Addressing the microplastic crisis: a multifaceted approach to removal and regulation, *Environ. Adv.*, 2024, **17**, 100579.
- 14 M. H. Milne, H. De Frond, C. M. Rochman, N. J. Mallos, G. H. Leonard and B. R. Baechler, Exposure of U.S. adults to microplastics from commonly-consumed proteins, *Environ. Pollut.*, 2024, **343**, 123233.
- 15 A. L. Andrady, Microplastics in the marine environment, *Mar. Pollut. Bull.*, 2011, **62**, 1596–1605.
- 16 I. M. Jaikumar, M. Tomson, A. Meyyazhagan, B. Balamuralikrishnan, R. Baskaran, M. Pappuswamy, H. Kamyab, E. Khalili and M. Farajnezhad, A comprehensive review of microplastic pollution in freshwater and marine environments, *Green Anal. Chem.*, 2025, **12**, 100202.
- 17 K. D. Cox, G. A. Covernton, H. L. Davies, J. F. Dower, F. Juanes and S. E. Dudas, Human consumption of microplastics, *Environ. Sci. Technol.*, 2019, **53**, 7068–7074.
- 18 S. A. Mason, V. G. Welch and J. Neratko, Synthetic polymer contamination in bottled water, *Front. Chem.*, 2018, **6**, 407.
- 19 A. J. Nihart, M. A. Garcia, E. El Hayek, R. Liu, M. Olewine, J. D. Kingston, E. F. Castillo, R. R. Gullapalli, T. Howard, B. Bleske, J. Scott, J. Gonzalez-Estrella, J. M. Gross, M. Spilde, N. L. Adolphi, D. F. Gallego, H. S. Jarrell, G. Dvorscak, M. E. Zuluaga-Ruiz, A. B. West and M. J. Campen, Bioaccumulation of microplastics in decedent human brains, *Nat. Med.*, 2025, **31**, 1114–1119.
- 20 L. C. Jenner, J. M. Rotchell, R. T. Bennett, M. Cowen, V. Tentzeris and L. R. Sadofsky, Detection of microplastics in human lung tissue using  $\mu$ FTIR spectroscopy, *Sci. Total Environ.*, 2022, **831**, 154907.
- 21 A. Ragusa, A. Svelato, C. Santacroce, P. Catalano, V. Notarstefano, O. Carnevali, F. Papa, M. C. A. Rongioletti, F. Baiocco, S. Draghi, E. D'Amore, D. Rinaldo, M. Matta and E. Giorgini, Plasticenta: first evidence of microplastics in human placenta, *Environ. Int.*, 2021, **146**, 106274.
- 22 T. Narancic and K. E. O'Connor, Plastic waste as a global challenge: are biodegradable plastics the answer to the plastic waste problem?, *Microbiology*, 2019, **165**, 129–137.
- 23 L. Zimmermann, Z. Bartosova, K. Braun, J. Oehlmann, C. Völker and M. Wagner, Plastic products leach chemicals that induce *in vitro* toxicity under realistic use conditions, *Environ. Sci. Technol.*, 2021, **55**, 11814–11823.
- 24 H. Çobanoğlu, M. Belivermiş, E. Sıkdokur, Ö. Kılıç and A. Çayır, Genotoxic and cytotoxic effects of polyethylene microplastics on human peripheral blood lymphocytes, *Chemosphere*, 2021, **272**, 129805.



- 25 S. Regmi, S. Paudel and S. Janaswamy, Packaging through the ages: a heuristic journey from leaves to plastics to cellulosic fibers and smart technologies, *Int. J. Biol. Macromol.*, 2025, **330**, 147885.
- 26 Z. Wu and M. Zhao, Hemicellulose, chitosan, and lignin-based biopolymer films for an improved and sustainable food packaging: a comprehensive review, *Int. J. Biol. Macromol.*, 2025, **319**, 145194.
- 27 T. Selvam, N. M. M. A. Rahman, F. Olivito, Z. Ilham, R. Ahmad and W. A. A. Q. I. Wan-Mohtar, Agricultural waste-derived biopolymers for sustainable food packaging: challenges and future prospects, *Polymers*, 2025, **17**, 1897.
- 28 M. E. González-López, S. de J. Calva-Estrada, M. S. Gradilla-Hernández and P. Barajas-Álvarez, Current trends in biopolymers for food packaging: a review, *Front. Sustainable Food Syst.*, 2023, **7**, 1225371.
- 29 Q. Xu, C. Chen, K. Rosswurm, T. Yao and S. Janaswamy, A facile route to prepare cellulose-based films, *Carbohydr. Polym.*, 2016, **149**, 274–281.
- 30 S. Janaswamy, M. P. Yadav, M. Hoque, S. Bhattarai and S. Ahmed, Cellulosic fraction from agricultural biomass as a viable alternative for plastics and plastic products, *Ind. Crops Prod.*, 2022, **179**, 114692.
- 31 S. Paudel, S. Regmi and S. Janaswamy, Effect of glycerol and sorbitol on cellulose-based biodegradable films, *Food Packag. Shelf Life*, 2023, **37**, 101090.
- 32 S. Paudel and S. Janaswamy, Corn-cob-derived biodegradable packaging films: a sustainable solution for raspberry post-harvest preservation, *Food Chem.*, 2024, **454**, 139749.
- 33 S. Regmi and S. Janaswamy, Biodegradable films from soyhull cellulosic residue with UV protection and antioxidant properties improve the shelf-life of post-harvested raspberries, *Food Chem.*, 2024, **460**, 140672.
- 34 S. Paudel, S. Regmi and S. Janaswamy, Valorization of biowaste to biopackaging: development of biodegradable films from cow dung-derived cellulose, *Biomass Bioenergy*, 2026, **204**, 108443.
- 35 S. Paudel, S. Regmi, S. Bhattarai, A. Fennell and S. Janaswamy, Valorization of grapevine agricultural waste into transparent and high-strength biodegradable films for sustainable packaging, *Sustainable Food Technol.*, 2025, **3**, 1218–1231.
- 36 S. Bhattarai and S. Janaswamy, Biodegradable films from the lignocellulosic residue of switchgrass, *Resour., Conserv. Recycl.*, 2024, **201**, 107322.
- 37 M. Soofi, A. Alizadeh, H. Hamishehkar, H. Almasi and L. Roufegarinejad, Preparation of nanobiocomposite film based on lemon waste containing cellulose nanofiber and savory essential oil: a new biodegradable active packaging system, *Int. J. Biol. Macromol.*, 2021, **169**, 352–361.
- 38 J. S. Yaradoddi, N. R. Banapurmath, S. V. Ganachari, M. E. M. Soudagar, N. M. Mubarak, S. Hallad, S. Hugar and H. Fayaz, Biodegradable carboxymethyl cellulose based material for sustainable packaging application, *Sci. Rep.*, 2020, **10**, 21960.
- 39 S. Paudel and S. Janaswamy, Use of alfalfa cellulose for formulation of strong, biodegradable film to extend the shelf life of strawberries, *Int. J. Biol. Macromol.*, 2025, **290**, 139004.
- 40 B. B. Sedayu, M. J. Cran and S. W. Bigger, A review of property enhancement techniques for carrageenan-based films and coatings, *Carbohydr. Polym.*, 2019, **216**, 287–302.
- 41 B. Kokkuvayil Ramadas, J.-W. Rhim and S. Roy, Recent progress of carrageenan-based composite films in active and intelligent food packaging applications, *Polymers*, 2024, **16**, 1001.
- 42 X. Wang, C. Guo and H. Guo, Progress of carrageenan-based films and coatings for food packaging applications, *Packag. Technol. Sci.*, 2024, **37**, 533–550.
- 43 G. Genecya, D. R. Adhika, W. Sutrisno and T. D. K. Wungu, Characteristic improvement of a carrageenan-based bionanocomposite polymer film containing montmorillonite as food packaging through the addition of silver and cerium oxide nanoparticles, *ACS Omega*, 2023, **8**, 39194–39202.
- 44 M. Dmitrenko, D. Pasquini, M. P. Bernardo, J. M. de Lima Alves, A. Kuzminova, I. Dzhakashov, A. Terentyev, A. Dyachkov, K. S. Joshy, M. J. John, S. Thomas and A. Penkova, Bio-composite films from carrageenan/starch reinforced with nanocellulose for active edible food packaging: development and optimization, *J. Renewable Mater.*, 2025, **13**, 1139–1168.
- 45 S. Sabu Mathew, A. K. Jaiswal and S. Jaiswal, Carrageenan-based sustainable biomaterials for intelligent food packaging: a review, *Carbohydr. Polym.*, 2024, **342**, 122267.
- 46 G. A. Paula, N. M. B. Benevides, A. P. Cunha, A. V. de Oliveira, A. M. B. Pinto, J. P. S. Morais and H. M. C. Azeredo, Development and characterization of edible films from mixtures of  $\kappa$ -carrageenan,  $\iota$ -carrageenan, and alginate, *Food Hydrocolloids*, 2015, **47**, 140–145.
- 47 G. Genecya, D. R. Adhika, Widayani and T. D. K. Wungu, Optimization of mechanical properties of carrageenan-based bioplastic as food packaging, *IOP Conf. Ser. Earth Environ. Sci.*, 2023, **1201**, 012079.
- 48 C. Santos, A. Ramos, Á. Luís and M. E. Amaral, Production and characterization of  $\kappa$ -carrageenan films incorporating *Cymbopogon winterianus* essential oil as new food packaging materials, *Foods*, 2023, **12**, 2169.
- 49 C. Cheng, S. Chen, J. Su, M. Zhu, M. Zhou, T. Chen and Y. Han, Recent advances in carrageenan-based films for food packaging applications, *Front. Nutr.*, 2022, **9**, 1004588.
- 50 B. T. Nguyen, T. Nicolai, L. Benyahia and C. Chassenieux, Synergistic effects of mixed salt on the gelation of  $\kappa$ -carrageenan, *Carbohydr. Polym.*, 2014, **112**, 10–15.
- 51 M. Huang, Y. Mao, H. Li and H. Yang, Kappa-carrageenan enhances the gelation and structural changes of egg yolk via electrostatic interactions with yolk protein, *Food Chem.*, 2021, **360**, 129972.
- 52 L. Wang, Y. Cao, K. Zhang, Y. Fang, K. Nishinari and G. O. Phillips, Hydrogen bonding enhances the electrostatic complex coacervation between  $\kappa$ -carrageenan and gelatin, *Colloids Surf., A*, 2015, **482**, 604–610.



- 53 S. Janaswamy and R. Chandrasekaran, Sodium ι-carrageenan: a paradigm of polymorphism and pseudopolymorphism, *Macromolecules*, 2006, **39**, 3345–3349.
- 54 S. Janaswamy and R. Chandrasekaran, Cation-induced polymorphism in iota-carrageenan, *Carbohydr. Polym.*, 2005, **60**, 499–505.
- 55 S. Janaswamy and R. Chandrasekaran, Three-dimensional structure of the sodium salt of iota-carrageenan, *Carbohydr. Res.*, 2001, **335**, 181–194.
- 56 A. A. Abdillah and A. L. Charles, Characterization of a natural biodegradable edible film obtained from arrowroot starch and iota-carrageenan and application in food packaging, *Int. J. Biol. Macromol.*, 2021, **191**, 618–626.
- 57 J. Zhao, C. Sun, H. Li, X. Dong and X. Zhang, Studies on the physicochemical properties, gelling behavior and drug release performance of agar/κ-carrageenan mixed hydrogels, *Int. J. Biol. Macromol.*, 2020, **154**, 878–887.
- 58 R. Stenner, N. Matubayasi and S. Shimizu, Gelation of carrageenan: effects of sugars and polyols, *Food Hydrocolloids*, 2016, **54**, 284–292.
- 59 Z. Yang, H. Yang and H. Yang, Effects of sucrose addition on the rheology and microstructure of κ-carrageenan gel, *Food Hydrocolloids*, 2018, **75**, 164–173.
- 60 H. Tao, L. Guo, Z. Qin, B. Yu, Y. Wang, J. Li, Z. Wang, X. Shao, G. Dou and B. Cui, Textural characteristics of mixed gels improved by structural recombination and the formation of hydrogen bonds between curdlan and carrageenan, *Food Hydrocolloids*, 2022, **129**, 107678.
- 61 G. Hernández-Carmona, Y. Freile-Peigrín and E. Hernández-Garibay, in *Functional Ingredients from Algae for Foods and Nutraceuticals*, Elsevier, 2013, pp. 475–516.
- 62 L. Piculell, *Food Polysaccharides and Their Applications*, Marcel Dekker, Inc., New York, 1995, pp. 205–244.
- 63 G. H. Therkelsen, in *Industrial Gums: Polysaccharides and Their Derivatives*, Academic Press, New York, 1993, pp. 145–180.
- 64 A. R. Barman, P. P. Dutta, K. Kapila, K. K. Bania and D. J. Haloi, Synergistic effect of glycerol and calcium chloride on the properties of cellulose acetate film, *J. Appl. Polym. Sci.*, 2024, **142**, e56615.
- 65 S. Regmi and S. Janaswamy, Biodegradable packaging films from the alkali-extracted lignocellulosic residue of soyhulls extend the shelf life of strawberries, *Food Biosci.*, 2025, **65**, 106016.
- 66 S. Regmi, S. Paudel and S. Janaswamy, Development of eco-friendly packaging films from soyhull lignocellulose: towards valorizing agro-industrial byproducts, *Foods*, 2024, **4000**.
- 67 S. Bhattarai and S. Janaswamy, Biodegradable, UV-blocking, and antioxidant films from lignocellulosic fibers of spent coffee grounds, *Int. J. Biol. Macromol.*, 2023, **253**, 126798.
- 68 S. Paudel and S. Janaswamy, Green valorization of alfalfa into sustainable lignocellulosic films for packaging applications, *Appl. Sci.*, 2025, **15**, 11889.
- 69 S. Ahmed and S. Janaswamy, Green fabrication of biodegradable films: harnessing the cellulosic residue of oat straw, *Int. J. Biol. Macromol.*, 2025, **303**, 140656.
- 70 Y. Tang, K. Lu, L. Lu, X. Qiu and L. Pan, Converting poplar sawdust waste into antioxidant lignocellulose film, *Biomass Convers. Biorefin.*, 2025, **15**, 22651–22661.
- 71 S. Bhattarai and S. Janaswamy, Biodegradable, UV-blocking, and antioxidant films from alkali-digested lignocellulosic residue fibers of switchgrass, *Chemosphere*, 2024, **359**, 142393.
- 72 K. Alba and V. Kontogiorgos, in *Encyclopedia of Food Chemistry*, Elsevier, 2019, pp. 240–250.
- 73 L. Li, R. Ni, Y. Shao and S. Mao, Carrageenan and its applications in drug delivery, *Carbohydr. Polym.*, 2014, **103**, 1–11.
- 74 Y. Dong, Z. Wei and C. Xue, Recent advances in carrageenan-based delivery systems for bioactive ingredients: a review, *Trends Food Sci. Technol.*, 2021, **112**, 348–361.
- 75 B. Neamtu, A. Barbu, M. O. Negrea, C. Ștefan Berghean-Neamțu, D. Popescu, M. Zăhan and V. Mireșan, Carrageenan-based compounds as wound healing materials, *Int. J. Mol. Sci.*, 2022, **23**, 9117.
- 76 J. Necas and Bartosikova, Carrageenan: a review, *Vet. Med.*, 2013, **58**, 187–205.
- 77 S. Ahmed and S. Janaswamy, Strong and biodegradable films from avocado peel fiber, *Ind. Crops Prod.*, 2023, **201**, 116926.
- 78 S. Ahmed, S. Janaswamy and M. P. Yadav, Biodegradable films from the lignocellulosic fibers of wheat straw biomass and the effect of calcium ions, *Int. J. Biol. Macromol.*, 2024, **264**, 130601.
- 79 G. A. M. de Jesus, S. B. R. Berton, B. M. Simões, R. S. Zola, J. P. Monteiro, A. F. Martins and E. G. Bonafé, κ-Carrageenan/poly(vinyl alcohol) functionalized films with gallic acid and stabilized with metallic ions, *Int. J. Biol. Macromol.*, 2023, **253**, 127087.
- 80 L. Qiu, Q. Luo, C. Bai, G. Xiong, S. Jin, H. Li and T. Liao, Preparation and characterization of a biodegradable film using irradiated chitosan incorporated with lysozyme and carrageenan and its application in crayfish preservation, *Foods*, 2023, **12**, 2642.
- 81 R. Mavelil-Sam, E. M. Ouseph, M. Morreale, R. Scaffaro and S. Thomas, Recent developments and formulations for hydrophobic modification of carrageenan bionanocomposites, *Polymers*, 2023, **15**, 1650.
- 82 M. Hoque and S. Janaswamy, Biodegradable packaging films from banana peel fiber, *Sustainable Chem. Pharm.*, 2024, **37**, 101400.
- 83 O. N. Pozharitskaya, A. N. Shikov, D. V. Demchenko, E. V. Flisyuk, V. G. Makarov and S. S. C. Academy, Effect of plasticizers on moisture absorption and mechanical properties of agar films, *Pharmacy*, 2017, **8**, 18–23.
- 84 M. Goma, A. A. Al-Badaani, A. F. Hifney and M. S. Adam, Utilization of cellulose and ulvan from the green seaweed *Ulva lactuca* in the development of composite edible films with natural antioxidant properties, *J. Appl. Phycol.*, 2022, **2615–2626**.
- 85 FAO, *Carrageenan*, [http://fao.org/fileadmin/user\\_upload/jecfa\\_additives/docs/monograph16/additive-117-m16.pdf](http://fao.org/fileadmin/user_upload/jecfa_additives/docs/monograph16/additive-117-m16.pdf), accessed 25 October 2025.



- 86 S. Tripathi, L. Kumar, R. K. Deshmukh and K. K. Gaikwad, Ultraviolet blocking films for food packaging applications, *Food Bioprocess Technol.*, 2024, **17**, 1563–1582.
- 87 H. Suryanto, E. Marsyahyo, Y. S. Irawan and R. Soenoko, Morphology, structure, and mechanical properties of natural cellulose fiber from Mendong grass (*Fimbristylis globulosa*), *J. Nat. Fibers*, 2014, **11**, 333–351.
- 88 J. Prado-Fernández, J. A. Rodríguez-Vázquez, E. Tojo and J. M. Andrade, Quantitation of  $\kappa$ -,  $\iota$ - and  $\lambda$ -carrageenans by mid-infrared spectroscopy and PLS regression, *Anal. Chim. Acta*, 2003, **480**, 23–37.
- 89 M. Sekkal, P. Legrand, J. P. Huvenne and M. C. Verdus, The use of FTIR microspectrometry as a new tool for the identification *in situ* of polygalactanes in red seaweeds, *J. Mol. Struct.*, 1993, **294**, 227–230.
- 90 T. Chopin and E. Whalen, A new and rapid method for carrageenan identification by FT IR diffuse reflectance spectroscopy directly on dried, ground algal material, *Carbohydr. Res.*, 1993, **246**, 51–59.
- 91 M. Sekkal and P. Legrand, A spectroscopic investigation of the carrageenans and agar in the 1500–100  $\text{cm}^{-1}$  spectral range, *Spectrochim. Acta, Part A*, 1993, **49**, 209–221.
- 92 R. H. Wilson, B. J. Goodfellow and P. S. Belton, Fourier transform infrared spectroscopy for the study of food biopolymers, *Food Hydrocolloids*, 1988, **2**, 169–178.
- 93 P. S. Belton, B. J. Goodfellow and R. H. Wilson, A variable-temperature Fourier-transform infrared study of gelation in  $\iota$ - and  $\kappa$ -carrageenans, *Macromolecules*, 1989, **22**, 1636–1642.
- 94 P. S. Belton, R. H. Wilson and D. H. Chenery, Interaction of group I cations with iota and kappa carrageenans studied by Fourier transform infrared spectroscopy, *Int. J. Biol. Macromol.*, 1986, **8**, 247–251.
- 95 N. Rajasulochana and S. Gunasekaran, Analysis on the seasonal variations in carrageenans of *Hypnea flagelliformis* and *Sarconema filiforme* by FTIR spectroscopy, *Asian J. Chem.*, 2009, **21**, 4547–4552.
- 96 X.-T. Ma, X.-Y. Sun, K. Yu, B.-S. Gui, Q. Gui and J.-M. Ouyang, Effect of content of sulfate groups in seaweed polysaccharides on antioxidant activity and repair effect of subcellular organelles in injured HK-2 cells, *Oxid. Med. Cell. Longevity*, 2017, **2017**, 2542950.
- 97 S. Daei, F. Mohtarami and S. Pirsá, A biodegradable film based on carrageenan gum/*Plantago psyllium* mucilage/red beet extract: physicochemical properties, biodegradability and water absorption kinetic, *Polym. Bull.*, 2022, **79**, 11317–11338.
- 98 M. Mahardika, M. V. Jatul Fitri, Y. Kusumastuti, L. Suryanegara, Fitriani, D. Amelia, Holilah, S. M. Sapuan, V. U. Siddiqui and M. K. Mohamad Haafiz, Effect of plasticizer on biodegradability, physical, and morphological properties of  $\kappa$ -carrageenan biopolymer films, *Biomass Bioenergy*, 2025, **201**, 108096.

